Simultaneous atmospheric nitrous oxide, methane and water vapor detection with a single continuous wave quantum cascade laser

Yingchun Cao,[1,*] Nancy P. Sanchez,[2] Wenzhe Jiang,[1] Robert J. Griffin,[2] Feng Xie,[3] Lawrence C. Hughes,[3] Chung-en Zah,[3] and Frank K. Tittel[1]

[1] *Department of Electrical and Computer Engineering, Rice University, 6100 Main Street, Houston, TX 77005, USA*
[2] *Department of Civil and Environmental Engineering, Rice University, 6100 Main Street, Houston, TX 77005, USA*
[3] *Corning Incorporated, Corning, New York 14831, USA*
[*] *yc62@rice.edu*

Abstract: A continuous wave (CW) quantum cascade laser (QCL) based absorption sensor system was demonstrated and developed for simultaneous detection of atmospheric nitrous oxide (N_2O), methane (CH_4), and water vapor (H_2O). A 7.73-μm CW QCL with its wavelength scanned over a spectral range of 1296.9-1297.6 cm^{-1} was used to simultaneously target three neighboring strong absorption lines, N_2O at 1297.05 cm^{-1}, CH_4 at 1297.486 cm^{-1}, and H_2O at 1297.184 cm^{-1}. An astigmatic multipass Herriott cell with a 76-m path length was utilized for laser based gas absorption spectroscopy at an optimum pressure of 100 Torr. Wavelength modulation and second harmonic detection was employed for data processing. Minimum detection limits (MDLs) of 1.7 ppb for N_2O, 8.5 ppb for CH_4, and 11 ppm for H_2O were achieved with a 2-s integration time for individual gas detection. This single QCL based multi-gas detection system possesses applications in environmental monitoring and breath analysis.

OCIS codes: (280.3420) Laser sensors; (010.1280) Atmospheric composition; (300.6340) Spectroscopy, infrared; (140.5965) Semiconductor lasers, quantum cascade.

References and links

1. T. F. Stocker, D. Qin, G.-K. Plattner, M. Tignor, S. K. Allen, J. Boschung, A. Nauels, Y. Xia, V. Bex and P. M. Midgley, *Climate Change 2013: The Physical Science Basis* (Cambridge University, Cambridge, United Kingdom and New York, NY, USA, 2013).
2. S. A. Montzka, E. J. Dlugokencky, and J. H. Butler, "Non-CO_2 greenhouse gases and climate change," Nature **476**, 43-50 (2011).
3. P. C. Castillo, I. Sydoryk, B. Gross, and F. Moshary, "Ambient detection of CH_4 and N_2O by Quantum Cascade Laser," Proc. of SPIE **8718**, 87180J (2013).
4. D. D. Nelson, B. McManus, S. Urbanski, S. Herndon, and M. S. Zahniser, "High precision measurements of atmospheric nitrous oxide and methane using thermoelectrically cooled mid-infrared quantum cascade lasers and detectors," Spectrochim. Acta. A. Mol. **60**, 3325-3335 (2004).
5. J. J. Scherer, J. B. Paul, H. J. Jost, and M. L. Fischer, "Mid-IR difference frequency laser-based sensors for ambient CH_4, CO, and N_2O monitoring," Appl. Phys. B **110**(2), 271-277 (2013).
6. L. Tao, K. Sun, M. A. Khan, D. J. Miller, and M. A. Zondlo, "Compact and portable open-path sensor for simultaneous measurements of atmospheric N_2O and CO using a quantum cascade laser," Opt. Express **20**(27), 28106-28118 (2012).
7. I. Mappé, L. Joly, G. Durry, X. Thomas, T. Decarpenterie, J. Cousin, N. Dumelie, E. Roth, A. Chakir, and P. G. Grillon, "A quantum cascade laser absorption spectrometer devoted to the in situ measurement of atmospheric N_2O and CH_4 emission fluxes," Rev. Sci. Instrum. **84**, 023103 (2013).
8. M. Jahjah, W. Ren, P. Stefański, R. Lewicki, J. Zhang, W. Jiang, J. Tarka, and F. K. Tittel, "A compact QCL based methane and nitrous oxide sensor for environmental and medical applications," Analyst **139**, 2065-2069 (2014).

9. W. Ren, W. Jiang, and F. K. Tittel, "Single-QCL-based absorption sensor for simultaneous trace-gas detection of CH_4 and N_2O," Appl. Phys. B **117**(1), 245-251 (2014).
10. D. L. Bjorneberg, A. B. Leytem, D. T. Westermann, P. R. Griffiths, L. Shao, and M. J. Pollard, "Measurement of atmospheric ammonia, methane, and nitrous oxide at a concentrated dairy production facility in Southern Idaho using open-path FTIR spectrometry," Transactions of the ASABE. **52**(5), 1749-1756 (2009).
11. S. N. Vardag, S. Hammer, S. O'Doherty, T. G. Spain, B. Wastine, A. Jordan, and I. Levin, "Comparisons of continuous atmospheric CH_4, CO_2 and N_2O measurements - results from a travelling instrument campaign at Mace Head," Atmos. Chem. Phys. **14**, 8403-8418 (2014).
12. L. S. Rothman, I. E. Gordon, A. Barbe, D. Chris Benner, P. F. Bernath, M. Birk, V. Boudon, L. R. Brown, A. Campargue, J.-P. Champion, K. Chance, L. H. Coudert, V. Dana, V. M. Devi, S. Fally, J.-M. Flaud, R. R. Gamache, A. Goldman, D. Jacquemart, I. Kleiner, N. Lacome, W. J. Lafferty, J.-Y. Mandin, S. T. Massie, S. N. Mikhailenko, C. E. Miller, N. Moazzen-Ahmadi, O. V. Naumenko, A. V. Nikitin, J. Orphal, V. I. Perevalov, A. Perrin, A. Predoi-Cross, C. P. Rinsland, M. Rotger, M. Šimečková, M. A. H. Smith, K. Sung, S. A. Tashkun, J. Tennyson, R. A. Toth, A. C. Vandaele, and J. Vander Auwera, "The HITRAN 2008 molecular spectroscopic database," J. Quant. Spectrosc. Radiat. Transf. **110**(9-10), 533-572 (2009).
13. M. Zahniser, "Nitrous Oxide Monitors", http://www.aerodyne.com/products/nitrous-oxide-monitors.
14. J. Faist, F. Capasso, D. L. Sivco, C. Sirtori, A. L. Hutchinson, and A. Y. Cho, "Quantum cascade laser," Science **264**(5158), 553-556 (1994).
15. M. Beck, D. Hofstetter, T. Aellen, J. Faist, U. Oesterle, M. Ilagems, E. Gini, and H. Melchior, "Continuous wave operation of a mid-infrared semiconductor laser at room temperature," Science **295**, 301-305 (2002).
16. J. Faist, *Quantum Cascade Lasers*, (Oxford University Press, UK, 2013).
17. A. Kosterev, G. Wysocki, Y. Bakhirkin, S. So, R. Lewicki, M. Fraser, F. Tittel, and R.F. Curl, "Application of quantum cascade lasers to trace gas analysis," Appl. Phys. B **90**(2), 165-176 (2008).
18. A. A. Kosterev, Y. A. Bakhirkin, and F. K. Tittel, "Ultrasensitive gas detection by quartz-enhanced photoacoustic spectroscopy in the fundamental molecular absorption bands region," Appl. Phys. B **80**(1), 133-138 (2005).
19. G. Wysocki, Y. A Bakhirkin, S. So, F. K. Tittel, C. J. Hill, R. Q. Yang, and M. P. Fraser, "Dual interband cascade laser based trace-gas sensor for environmental monitoring," Appl. Opt. **46**(33), 8202-8210 (2007).
20. M. Jahjah, W. Jiang, N. P. Sanchez, W. Ren, P. Patimisco, V. Spagnolo, S.C. Herndon, R.J. Griffin, and F. K. Tittel, "Atmospheric CH_4 and N_2O measurements near Greater Houston are landfills using QCL based QEPAS sensor system during DISCOVER-AQ 2013," Opt. Lett. **39**(4), 957-960 (2014).
21. T. H. Risby and F. K. Tittel, "Current status of mid-infrared quantum and interband cascade lasers for clinical breath analysis," Opt. Eng. **49**(11), 111123-1-14 (2010).
22. R. Lewicki, A. A. Kosterev, D. M. Thomazy, T. H. Risby, S. Solga, T. B. Schwartz, and F. K. Tittel, "Real time ammonia detection in exhaled human breath using a distributed feedback quantum cascade laser based sensor." Proc. of SPIE **7945**, 50K-2 (2011).
23. J. B. McManus, P. L. Kebabian, and M. S. Zahniser, "Astigmatic mirror multipass absorption cells for long-path-length spectroscopy," Appl. Opt. **34**(18), 3336-3348 (1995).
24. F. A. Smith, S. Elliott, D. R. Blake, and F. S. Rowland, "Spatiotemporal variation of methane and other trace hydrocarbon concentration in the Valley of Mexico," Environ. Sci. Policy. **5**(6), 449-461 (2002).

1. Introduction

Nitrous oxide (N_2O), methane (CH_4), and water vapor (H_2O) are three major atmospheric greenhouse gases contributing to global warming and climate change [1, 2]. N_2O has a global warming potential (GWP) of 298 (100-yr horizon) and a longer atmospheric lifetime than carbon dioxide (CO_2) [1, 3]. Atmospheric N_2O concentrations are increasing at a rate of ~0.7

ppbv/yr and are currently approaching a 330 ppbv concentration level [1]. CH_4 has a relatively short lifetime (~12 years) in the atmosphere compared with CO_2 and N_2O, and exhibits a GWP of 25 (100-yr horizon) with atmospheric concentrations of ~1.8 ppm [3]. H_2O is a dominant energy carrier in the atmosphere and regulates planetary temperatures through absorption and emission of radiation [1]. Considering their environmental relevance, high precision and sensitivity measurements of these three greenhouse gases are necessary to determine their sources and concentration levels, leading to a better understanding of global warming and climate change.

The most widely used method for detection of atmospheric N_2O, CH_4 and H_2O is tunable diode laser absorption spectroscopy (TDLAS) [3-9]. Nelson et al. reported a compact and fast response mid-infrared absorption spectrometer for high precision N_2O and CH_4 measurements by using two different thermoelectrically cooled, pulsed quantum cascade lasers (QCLs) and a 56-m path-length multipass gas cell. Simultaneous measurements of N_2O and CH_4 with minimum detection limits (MDLs) of 3 ppb and 7 ppb were achieved respectively near 7.8 μm with a 1-s integration time [4]. Both laboratory and open path measurements for simultaneous detection of N_2O and CH_4 using a QCL were demonstrated. MDLs of 2 ppb for N_2O and 7 ppb for CH_4 at room temperature and atmospheric pressure based on a 210-m multipass cell have been reported [3]. Sensitive ambient CH_4, CO and N_2O measurements based on a single mid-infrared difference frequency generation laser system were performed with a 5-m multipass cell [5]. A compact and portable sensor was developed for simultaneous measurements of atmospheric N_2O and CO with a 4.5-μm QCL and an open-path multipass cell (16-m path-length, atmospheric pressure). Laboratory detection limits of 0.15 ppb for N_2O and 0.36 ppb for CO were achieved at 10 Hz [6]. A QCL absorption spectrometer was reported for in situ measurements of atmospheric N_2O and CH_4 emission fluxes [7]. A compact quartz-enhanced photoacoustic spectroscopy system was developed for CH_4 and N_2O detection with a 7.83-μm QCL. MDLs of 13 ppb and 6 ppb for CH_4 and N_2O were achieved with a 1-s data acquisition time [8]. A single-QCL based absorption sensor was demonstrated for simultaneous detection of ppb-level CH_4 and N_2O by using a 7.8-μm QCL and 57.6-m multipass cell, with MDLs of 5.9 ppb and 2.6 ppb for CH_4 and N_2O, respectively [9]. Other spectroscopic methods such as open-path Fourier transform infrared spectrometry [10] and cavity ring-down spectroscopy [11] have been reported for sensitive atmospheric multi-gas detection.

In this work, we developed an absorption sensor system for simultaneous atmospheric N_2O, CH_4, and H_2O concentration measurements by using a single continuous wave (CW) distributed feedback (DFB) QCL operating at a wavelength of ~7.71 μm. A commercially available multipass cell with a compact size (32 cm long, 0.5 liters volume) was used as the multi-gas absorption cell with an effective path length of 76 m.

2. Absorption line selection

Most atmospheric gas species have their strong fundamental absorption lines in the mid-infrared spectral range, which permits sensitive and selective atmospheric gases detection in this spectral range. Fig. 1(a) shows the absorption lines of three main atmospheric gases, i.e., N_2O, CH_4, and H_2O, for wavelengths from 3 to 8.5 μm based on the HITRAN database [12]. It can be observed that the strongest absorption bands are located at ~4.5 μm for N_2O, ~3.3 μm for CH_4, and ~5.9 μm for H_2O. However, there are relatively strong absorption lines for these three gases that overlap with each other at ~7.7 μm. This spectral feature makes feasible the simultaneous sensitive detection of three gases using a single QCL, thereby simplifying the sensor system and reducing its size and cost. A high-resolution absorption spectrum of our three selected gases at a pressure of 50 Torr and a 1-m absorption length is depicted in Fig. 1(b). Three neighboring absorption lines, a N_2O line at 1297.05 cm^{-1}, a CH_4 line at 1297.486 cm^{-1}, and a H_2O line at 1297.184 cm^{-1}, are well separated from each other within a relatively small spectral range of ~0.5 cm^{-1}. This allows a mid-infrared QCL operating at ~7.7 μm to cover three absorption lines simultaneously. It should be noted that the combination of these three lines might not be the only choice for simultaneous detection of N_2O, CH_4 and H_2O, but

is based on the operating wavelength range of the QCL that was available in our laboratory. For example, a laser frequency of 1270 cm^{-1} was selected for N_2O, H_2O and CH_4 detection by Aerodyne Research Inc. [13].

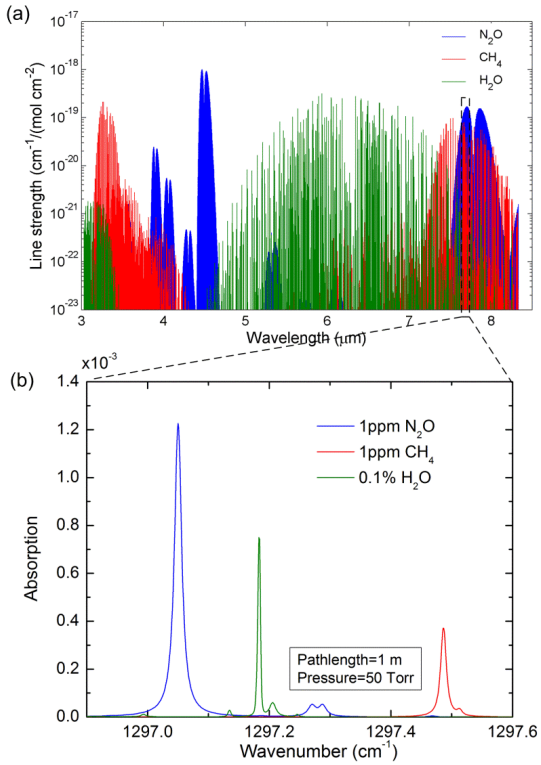

Fig. 1. (a) Absorption lines of N_2O, CH_4, and H_2O for a wide spectral range from 3 to 8.5 μm as vertical drop lines; (b) Absorption spectra of N_2O, CH_4, and H_2O in a narrow range from 1296.95 cm^{-1} to 1297.6 cm^{-1} for specific concentrations and a 1-m path length at a pressure of 50 Torr. N_2O, CH_4, and H_2O lines are shown as blue, red, and green, respectively.

3. Experimental

3.1 Characterization of QCL based TDLAS excitation source

Mid-infrared CW DFB QCLs are perfect excitation sources for laser-based gas sensor systems due to their operation in the spectral range covering most of the fundamental gas absorption lines, high optical power (>100 mW), relatively narrow linewidth, good wavelength tunability, ability to operate at room temperature and compact size [14-16]. Therefore, QCL-based gas sensor systems [17] are widely used for high sensitivity and selectivity trace gas detection in a variety of applications including environmental monitoring [18-20] and medical diagnostics [21,22]. A CW DFB-QCL (Corning Inc., New York) with a wavelength of ~7.73 μm was used as an excitation source to target the absorption lines near 1297 cm^{-1} for simultaneous multiple species gas detection. The QCL is enclosed in a high heat load (HHL) package, and the output QCL beam is collimated by an aspheric lens (f=1.87 mm) before passing through an antireflective Ge window that is used to seal the HHL package. The QCL output power and wavelength are measured using an optical power meter (NOVA II, OPHIR) and a Fourier transform infrared (FTIR) spectrometer (Nicolet 8700, Thermo Scientific), respectively. The optical power and wavenumber of the CW DFB QCL for different operating temperatures and injection currents are presented in Figs. 2(a) and 2(b), respectively. Fig. 2(b) shows that a wavenumber of ~1297 cm^{-1}, corresponding to the optimum target absorption spectral region for simultaneous detection of N_2O, CH_4, and H_2O, can be obtained at room

temperature and reduced current for this QCL. The current and temperature controlled wavelength tuning coefficients for this DFB-QCL are determined to be -0.014 cm^{-1}/mA and -0.09 cm^{-1}/°C, respectively. A QCL injection current of 240 mA combined with a 15 °C QCL operation temperature were selected for simultaneous atmospheric N_2O, CH_4 and H_2O concentration measurements.

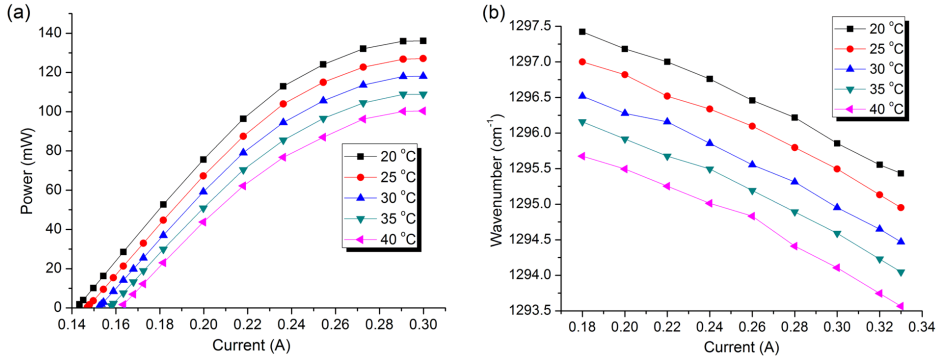

Fig. 2. Measured results for 7.73-µm CW DFB-QCL at different operating temperatures and injection currents. (a) QCL power response curves; (b) emitted wavenumber curves.

3.2 TDLAS based Sensor platform

A TDLAS method combined with a long path length gas absorption cell was utilized for multiple gas detection in this work. Wavelength modulation spectroscopy with second harmonic (2*f*-WMS) detection technique was adopted for data generation and processing to achieve an enhanced signal-to-noise ratio. The schematic setup of the sensor system is depicted in Fig. 3. A 7.73-µm CW DFB-QCL is operated with both a temperature controller (TED 200C, Thorlabs Inc.) and a current controller (LDX 3232, ILX Lightwave). The QCL beam was optimized and focused to the center of an astigmatic multipass gas cell (AMAC-76, Aerodyne Research Inc.) using a pair of plano-convex lenses (f_1=50 mm and f_2=100 mm) and a 400-µm-diameter pinhole. A visible diode laser (λ=630 nm) was injected into the system via a flip mirror and co-aligned with the infrared beam to facilitate the beam alignment with the multipass cell. When a desired beam pattern (shown in the upper-left corner of Fig. 3) appears on the front mirror of the cell, an effective path length of 76 m (238 passes) is achieved according to the AMAC-76 design specifications. The QCL beam exiting from the multipass cell was collected by a parabolic mirror and sent to a thermoelectrically (TE) cooled mid-infrared detector (PVMI-3TE-8, Vigo System S.A.). The QCL wavelength was tuned to the desired spectral range determined in Sect. 3.1 (240 mA, 15 °C), and then scanned and modulated by combined sawtooth and sinusoidal signals from a function generator (AFG 3102, Tektronix Inc.). The output signal from the detector was sent to a lock-in amplifier for second harmonic demodulation and recorded by a DAQ device. The DC part of the detector output was also recorded by the DAQ device via a low pass filter to monitor the laser power variation. The gas sample inside the multipass cell was controlled by a pressure controller (Type 640, MKS Instruments) and a vacuum pump (N813.5, KNF).

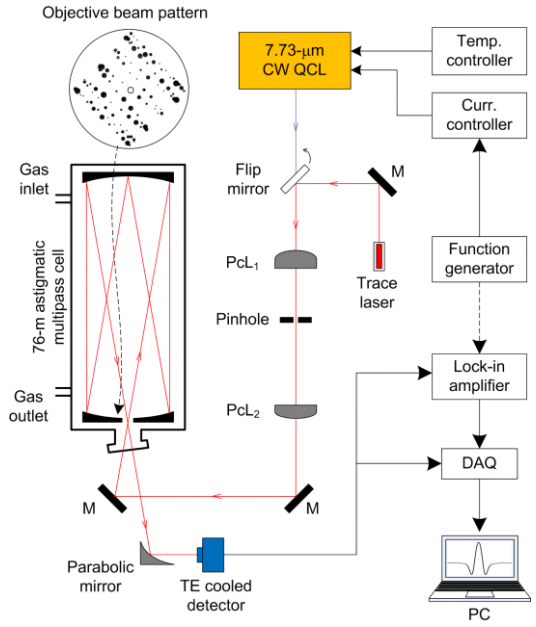

Fig. 3. Schematic of a three-gas sensor system based on a single CW DFB QCL. M: mirror; PcL: plano-convex lens; DAQ: data acquisition; PC: personal computer.

3.3 Flow response time test

The flow response time in the multipass gas cell was evaluated for N_2O, CH_4 and H_2O. The multipass gas cell was initially filled with a constant concentration of N_2O, CH_4, or H_2O. Pure dry N_2 was used to flush the cell at different flow rates. During this process, the signal at the absorption line peak of N_2O, CH_4, or H_2O was monitored. As different flow rates were injected into the multipass gas cell, the signal variation at the selected absorption lines for N_2O, CH_4, and H_2O was recorded accordingly. The amplitude-normalized signal for each individual gas during the flushing process is shown in Fig. 4. From Fig. 4, it is apparent that the flushing time decreases with increasing gas flow rate, which can be explained by the fact that a larger flow rate increases the gas exchange rate in the multipass gas cell. For a fixed flow rate, for example 140 standard cubic centimeters per minute (SCCM), the response times for N_2O, CH_4 and H_2O detection are estimated to be 4.8 s, 4.6 s, and 11.1 s, respectively from an exponential decay curve fitting on the curves shown in Fig. 4. These time response plots reveal that the removal rates of N_2O and CH_4 are comparable, while the response time for H_2O is significantly longer. This could be explained by the sticky nature of water molecules [23], i.e., the surface adsorption-desorption of water molecules inside the gas pipe and multipass cell greatly reduces the exchange rate of the water molecules.

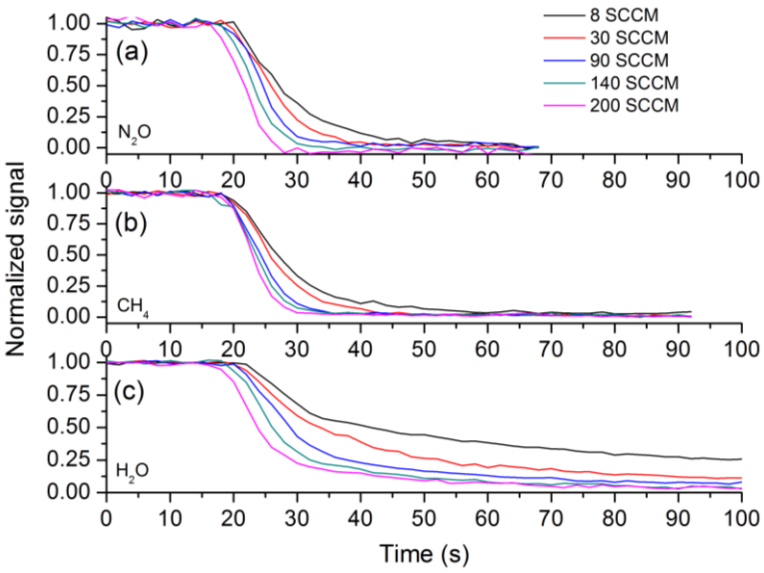

Fig. 4. Time response of (a) N_2O, (b) CH_4, and (c) H_2O detection with pure N_2 flushing at different gas flow rate. SCCM: standard cubic centimeters per minute.

4. Individual trace gas detection

The sensor system was first evaluated for individual trace gas detection in order to determine the MDLs for N_2O, CH_4, and H_2O. To this end, the CW DFB QCL wavelength was tuned to the respective N_2O, CH_4, and H_2O absorption line center to measure N_2O, CH_4, and H_2O concentrations individually.

4.1 N_2O detection

For N_2O detection, the QCL wavelength is tuned to the center of the target N_2O absorption line at ~1297.05 cm^{-1} (240 mA, 17.2 °C). A ramp signal (2 s in period, 6 mA in amplitude) is used to control the QCL wavelength scan. A 5 kHz sinusoidal signal is used to modulate the QCL wavelength and generate a 2*f* signal curve along the absorption line. The 2*f* signal is demodulated by a lock-in amplifier with an optimum time constant of 50 ms over the selected ramp period. In order to determine the optimum operating conditions for N_2O detection, the sensor system was evaluated at different pressures inside the multipass cell and WMS modulation depths. The peak 2*f* signals for a fixed N_2O concentration (330 ppb) were recorded for each individual pressure-modulation-depth combination and plotted in Fig. 5(a). Optimum operating conditions of 80 Torr and 4 mA were selected for N_2O concentration measurements.

The sensor calibration is performed by diluting gas from a standard cylinder containing 2 ppm N_2O balanced by N_2 with pure N_2. By controlling the flow rate of each cylinder, gas mixtures with different N_2O concentration levels ranging from 0 to 2 ppm are obtained precisely and delivered to the multipass gas cell for sensor sensitivity calibration. Figure 5(b) shows the 2*f* signal response of the sensor system when N_2O with different step concentration is injected into the gas cell. The signal plateaus for each concentration can be distinguished clearly, and the 2*f* signal shows good linear relationship (R^2=0.99774) with the concentration of N_2O, indicating a sensor sensitivity of 6.142 mV/ppm.

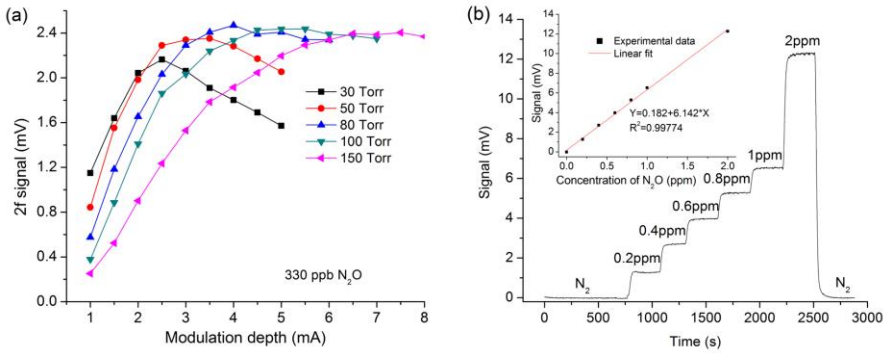

Fig. 5. (a) Pressure and modulation depth optimization for N_2O detection; (b) Sensor sensitivity calibration for N_2O. The inset of Fig. 5(b) shows the average signal for each N_2O concentration level and its linear fit.

The sensor detection limit of N_2O was determined by passing pure N_2 through the multipass gas cell at its optimum operating conditions. The 2*f* signal was recorded continuously with a time interval of 2 s over 500 s. The signal in terms of N_2O concentration based on the sensor sensitivity is presented in Fig. 6(a). An Allan deviation analysis was applied to evaluate the noise behavior for N_2O detection as depicted in Fig. 6(b). A MDL of 1.7 ppb for N_2O was observed for a 2-s sampling time, corresponding to a noise level of 1.7×10^{-4} in terms of absorption. This noise level results mainly from the laser controlling electronics. An optimum MDL is estimated to be 0.3 ppb for an integration time of 100 s.

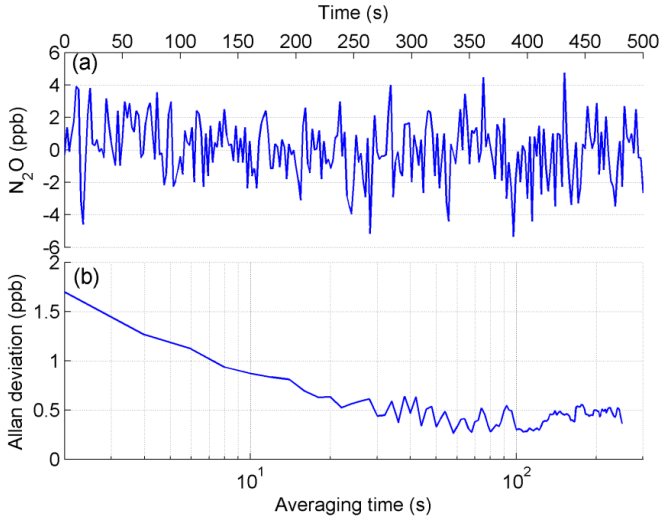

Fig. 6. (a) Measured N_2O concentration by passing pure N_2 into the multipass cell; (b) Allan deviation plot for the data shown in Fig. 6(a).

4.2 CH_4 detection

CH_4 detection is based on the strong absorption line of CH_4 at 1297.486 cm^{-1}. The QCL wavelength was tuned to the target line center (240 mA, 12.4 °C). A similar combined ramp (2 s, 10 mA) and sinusoidal signals (*f*=5 kHz) was applied to the CW QCL to realize laser wavelength scanning and modulation simultaneously as described in Sect. 4.1. The demodulated 2*f* signals at the absorption line peak with a lock-in time constant of 50 ms are plotted in Fig. 7(a) for different gas pressures in the multipass gas cell and modulation depths. According to Fig. 7(a), optimum operating conditions for the sensor system are found to be a

100-Torr pressure and 4-mA modulation depth. With these optimized sensor parameters, sensor calibration was carried out by using diluted standard CH_4 gas with different concentrations as shown in Fig. 7(b). The fitting curve in the inset of Fig. 7(b) indicates a good linear relationship (R^2=0.997) between 2*f* signal and CH_4 concentration, with a sensitivity of 3.137 mV/ppm.

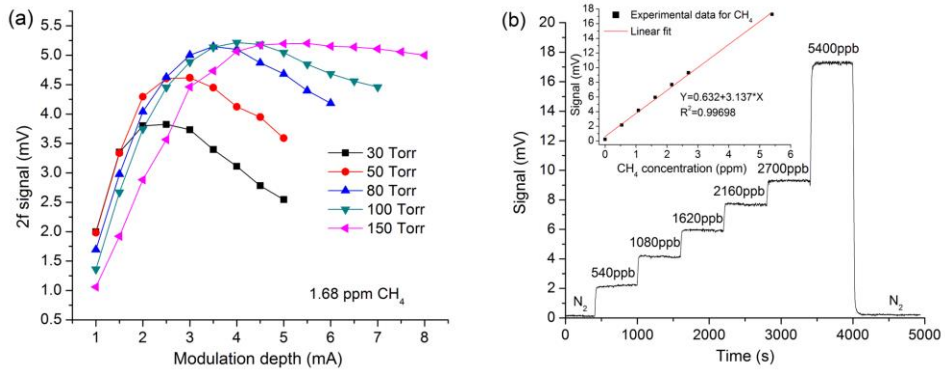

Fig. 7. (a) Pressure and modulation depth optimization for CH_4 detection; (b) CH_4 concentration response for the sensor system.

The noise level was determined by passing pure N_2 into the system and thereby subsequent monitoring the detected 2*f* signal in terms of CH_4 concentration at the CH_4 peak position based on the calibrated sensitivity for CH_4. Figure 8(a) shows the detected CH_4 concentration variation in the multipass gas cell over 800 s. A MDL of 8.5 ppb for CH_4 was achieved for a 2-s sampling time from the Allan deviation plot depicted in Fig. 8(b). This value can be improved to 2.5 ppb when the averaging time is increased to 50 s.

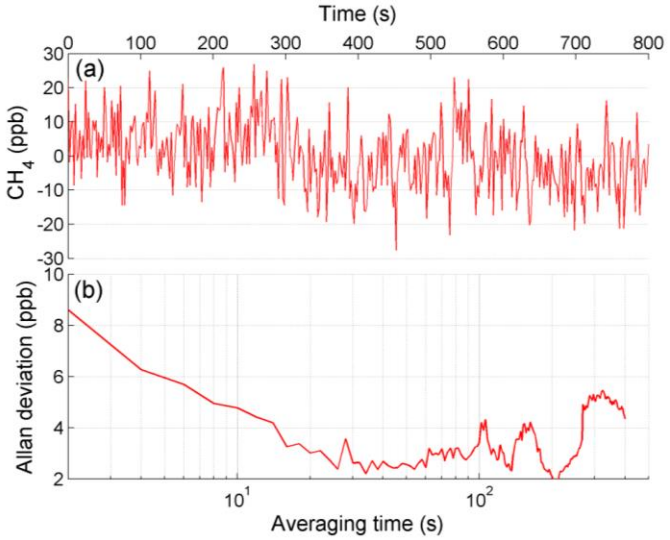

Fig. 8. (a) Measured CH_4 concentrations as pure N_2 flows over the multipass cell; (b) Allan deviation plot for the data in Fig. 8(a).

4.3 H_2O detection

The sensor system was also evaluated for H_2O detection. The water absorption line at 1297.184 cm^{-1} was selected as the target line, corresponding to the CW DFB QCL operating conditions of 240 mA and 15.7 °C. A 1-s ramp period and a 20-ms lock-in amplifier time

constant were applied for improved sensor performance. An optimum pressure of 400 Torr and modulation depth of 5.5 mA were determined for H_2O detection following the procedures described in Sect. 4.1 and 4.2. Considering the strong absorption for atmospheric H_2O, the water concentration in the multipass cell was calibrated by fitting the transmittance curve to theoretical simulations based on the HITRAN database [12]. The sensor was evaluated measuring a constant H_2O concentration generated by passing air flow over a container filled with deionized water. The results are displayed in Fig. 9(a) and reveal a measured average H_2O concentration in the multipass gas cell of 1.892%. From the Allan deviation analysis plot in Fig. 9(b), MDLs of 16 ppm with a 1-s integrating time and 11 ppm with a 2-s integrating time were obtained for H_2O measurement. An optimum MDL of 5 ppm can be estimated for an averaging time of 30 s.

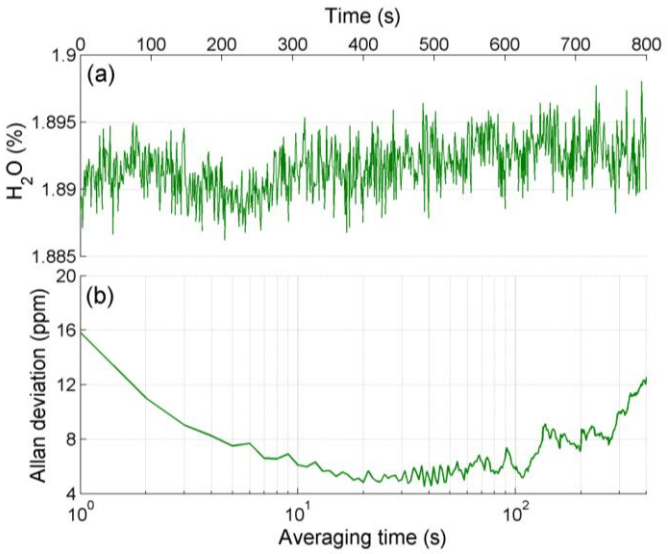

Fig. 9. (a) H_2O measurements during a 800 s period; (b) Allan deviation analysis.

5. Simultaneous three gas detection of N_2O, CH_4, and H_2O with a single CW QCL

As described in Sect. 2, the three neighboring strong absorption lines of N_2O, CH_4, and H_2O in a narrow spectral range of 1297-1297.5 cm^{-1} are monitored for simultaneous concentration measurements of these gases with a single QCL. The sensor system is the same used for individual gas detection as described in Sect. 4. A ramp signal with larger amplitude (11 mA, 1 Hz) was applied to the QCL with the heat sink temperature set to 20 ºC to cover all three absorption lines within a single continuous wavelength scan. A pressure of 100 Torr inside the multipass gas cell and a modulation depth of 4 mA were selected for optimum sensor operation. The direct output signal from the detector after a low pass filter is shown in Fig. 10(a) and the 2*f* signal demodulated by the lock-in amplifier with a time constant of 5 ms is depicted in Fig. 10(b) for ambient air. It is observed that these three gas lines are included with low interference within a single laser scan for both the absorption and 2*f* signals. In order to eliminate the effect of signal variation due to long term laser power drift, the measured 2*f* signal was normalized to the transmitted power as measured from the detector output in the non-absorption region. The N_2O and CH_4 sensitivity calibrations are based on the dilution of standard gases, and H_2O sensitivity is determined by dividing the normalized 2*f* signal by the H_2O concentration, which was obtained from the direct output curve of the detector as described in Sect. 4.3. The subsequent measurements are based on the analysis of the variation of these peaks for different gas concentration changes in a laboratory environment and ambient atmosphere, respectively.

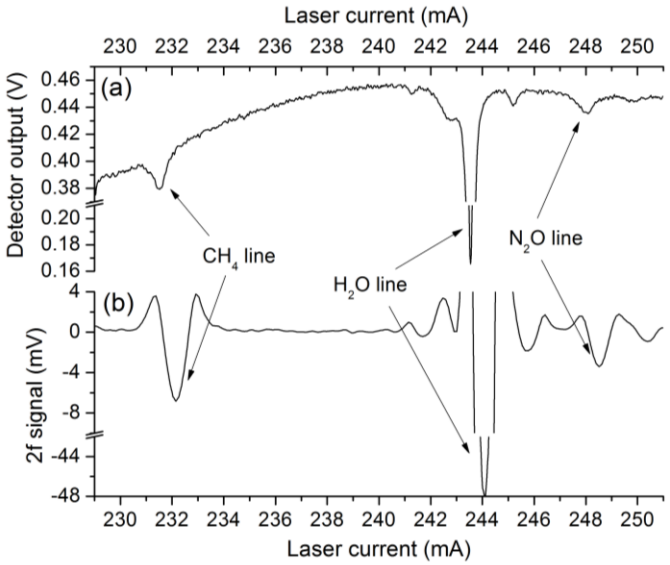

Fig. 10. (a) Direct output of the mid-infrared detector, and (b) 2*f* signal of the sensor system for simultaneous three gas species (N_2O, CH_4, and H_2O) detection at a pressure of 100 Torr and modulation depth of 4 mA.

5.1 Laboratory air component measurements

The sensor system was evaluated for simultaneous measurements of N_2O, CH_4, and H_2O concentrations in a laboratory environment. Measured concentration changes of N_2O, CH_4, and H_2O over 14 hours are displayed in Fig. 11(a). It is observed that the concentration of N_2O was relatively constant during this period of time, with a concentration level of ~345± 9.7 ppb. However, the CH_4 concentrations showed significant variation, from 2 ppm up to 4 ppm, especially in the early morning hours. This increase in the CH_4 concentration is in accordance with the typical diurnal profile exhibited by this gas species during summer time [24]. The H_2O concentrations were in the range of 0.86%-1.05%, with its maximum value appearing around 03:00 CDT. The average H_2O concentration during this period of time is found to be 0.97±0.046%. The MDLs of these three gases are analyzed for relatively stable concentration intervals within a continuous measurement period and plotted in Fig. 11(b). MDLs were found to be 6.5 ppb for N_2O, 23 ppb for CH_4, and 62 ppm for H_2O with a 1-s integration time. Compared with the individual gas detections described in Sect. 4, these MDLs are 3-4 times larger. This difference is mainly attributed to a larger wavelength scan range within a single ramp period of the sensor system for a 1 s acquisition time. However, with a longer averaging time of 100 s, the MDLs can be decreased to 0.4 ppb for N_2O, 3 ppb for CH_4 and 6 ppm for H_2O, which are appropriate for atmospheric concentration monitoring of these three species.

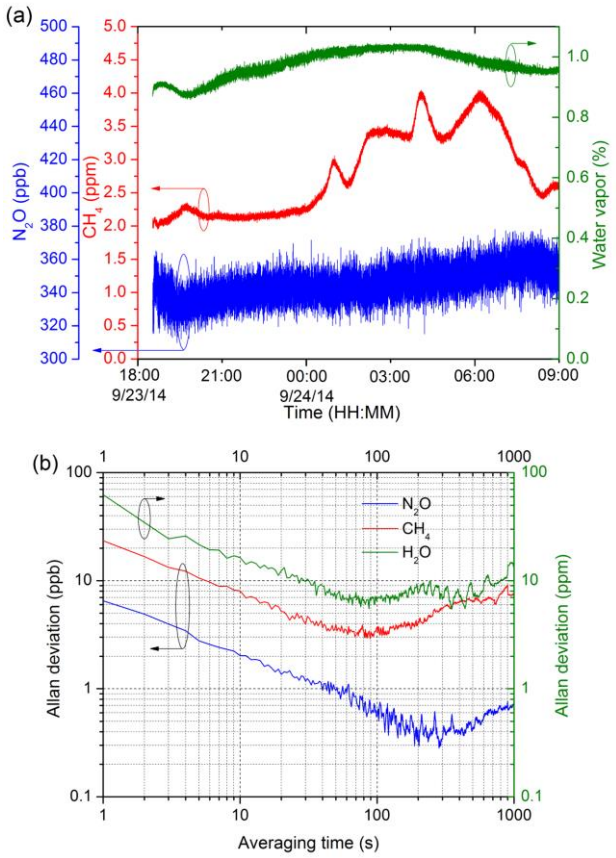

Fig. 11. (a) Simultaneously measured concentrations of N_2O, CH_4, and H_2O in laboratory ambient air; (b) Allan deviation of these three gases within constant concentration periods.

5.2 Atmospheric N_2O, CH_4, and H_2O concentration measurements

The sensor system was also evaluated for simultaneous three gas species detection present in the ambient atmosphere on the Rice University campus. The sensor system was installed on a cart and placed outside the Laser Science Laboratory to monitor variations of atmospheric N_2O, CH_4, and H_2O concentrations (Fig. 12(a)). The measured concentrations are plotted in Fig. 12(b). The experiment was conducted from 10:25 CDT to 16:35 CDT on September 24, 2014. At the end of the measurement period, pure N_2 was filled into the multipass cell to verify the zero-background signal. Concentration fluctuations were observed during atmospheric monitoring of N_2O, CH_4, and H_2O, especially for H_2O concentrations. For most of the sampling interval, the N_2O concentrations were in the range of 300-350 ppb, with an average value of 323±11 ppb. CH_4 concentrations were measured to be up to 4 ppm for the first 20 minutes (as reported in Sect. 5.1) of the monitoring period and then dropped gradually to its typical background level of ~1.87 ppm. The H_2O concentrations were found to be between 0.89% and 1.19%, with an average concentration of 0.99±0.039%. In order to examine the validity of these results, H_2O mixing ratios were calculated for the period of measurements based on local meteorological conditions (e.g. relative humidity, temperature and pressure). According to these calculations, H_2O concentration ranged between 0.74% and 0.98% with a mean value of 0.91±0.061% for the period between 10:25 CDT and 16:35 CDT on September 24, 2014. Although the estimated H_2O concentrations were slightly lower than those detected by the sensor system, good agreement was observed between both determinations. Additionally, detected N_2O and CH_4 levels are in accordance with the

corresponding atmospheric concentrations of these species [1, 3]. As shown in Fig. 12(b), pure N_2 flowing into the gas cell leads to a rapid decrease in the concentration signals of these three gas species.

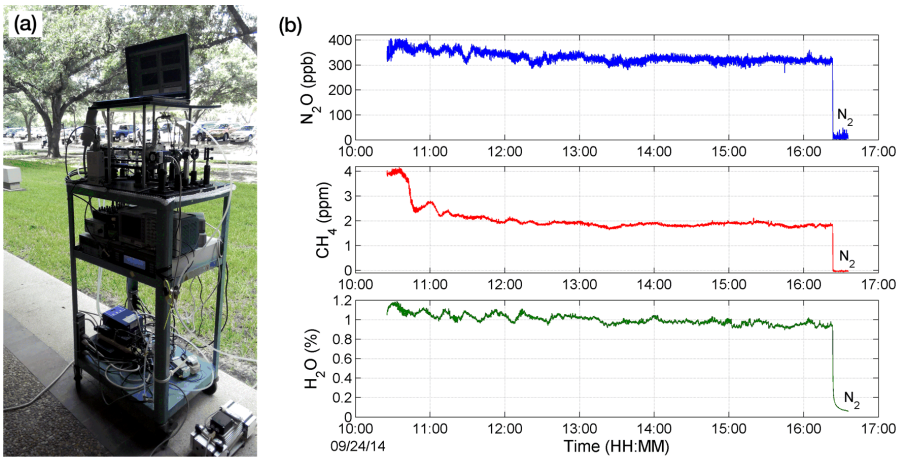

Fig. 12. (a) Single CW QCL based N_2O, CH_4 and H_2O sensor system; (b) Measurement results of simultaneous three gas concentrations monitoring in the atmosphere for a 6 hour time duration.

6. Conclusions

A sensitive and selective sensor system based on a single CW DFB-QCL was demonstrated for simultaneous detection of N_2O, CH_4 and H_2O. The system was based on TDLAS and 2*f*-WMS detection methods. A CW DFB-QCL with a wavelength of ~7.73 μm was employed to cover three strong absorption lines for different gas species within a narrow spectral range. An astigmatic multipass Herriott gas cell with an effective path length of 76 m was used to enhance the gas absorption in a compact space (0.5 liters). The sensor system was first evaluated for individual N_2O, CH_4, and H_2O detection, respectively, with the QCL wavelength tuned to each gas absorption line center. MDLs of 1.7 ppb for N_2O, 8.5 ppb for CH_4, and 11 ppm for H_2O with an integration time of 2 s were achieved for individual detection of these species. Subsequently, the sensor system was evaluated for simultaneous N_2O, CH_4, and H_2O detection based on this single QCL. Measurement results for both laboratory and atmospheric concentration changes of these three gases were presented and discussed. This system shows the advantage of simultaneous high-sensitivity multiple gas species detection with reduced cost and size.

Acknowledgments

We acknowledge the financial support from a National Science Foundation (NSF) ERC MIRTHE award, a NSF-ANR award for international collaboration in chemistry, "Next generation of Compact Infrared Laser based Sensor for Environmental Monitoring (NexCILAS)" and the Robert Welch Foundation grant C-0586.